MACHINING CONSIDERATIONS FOR WAAM PREFORMS

Jake Dvorak[1], Aaron Cornelius[1], Greg Corson[1], Ross Zameroski[1], Leah Jacobs[1], Joshua Penney[1], and Tony Schmitz[1,2]
[1]Department of Mechanical, Aerospace, and Biomedical Engineering
University of Tennessee, Knoxville
Knoxville, TN 37996, USA
[2]Manufacturing Science Division
Oak Ridge National Laboratory
Oak Ridge, TN, 37830, USA

ABSTRACT
Hybrid manufacturing consisting of metal additively manufactured preforms and computer numerical control (CNC) machining has been established to be an effective method for higher material use rates than traditional manufacturing methods. However, hybrid manufacturing introduces unique challenges. Near-net shape designs are typically selected, which results in a smaller margin for part placement within the stock. Consequently, when moving the workpiece between deposition and machining systems, the work coordinate system must be maintained to ensure part placement. Additionally, less stock material reduces the preform stiffness, which limits the material removal rates during machining. To date, a comprehensive digital twin methodology to accurately predict the machining outcome has not been presented.

KEYWORDS
Wire-arc additive, milling, hybrid manufacturing, fiducial, structured light scanning, machining dynamics

INTRODUCTION
The key topics of this research effort are hybrid manufacturing and the associated digital twin. While many digital twin descriptions are available [2-5], for the purposes of this study the working definition is: the digital counterpart, or twin, of a physical process that uses models and real-time data to predict the behavior of the physical process. Hybrid manufacturing encompasses a sequence of activities that integrate additive manufacturing (AM) with other processes. Here, AM + metrology + machining activities are used to produce the final part with geometry and surface finish that meet the designer's intent. The digital twin for this particular application of hybrid manufacturing includes:

- the AM material, parameters, and path used to fabricate the preform
- the preform geometry
- the preform structural dynamics
- the machining parameters and tool path
- the tool-holder-spindle-machine assembly structural dynamics
- a physics-based model to relate the preform material's cutting force model, preform and tool-holder-spindle-machine assembly structural dynamics, and milling stability [1]
- the final part geometry and surface finish.

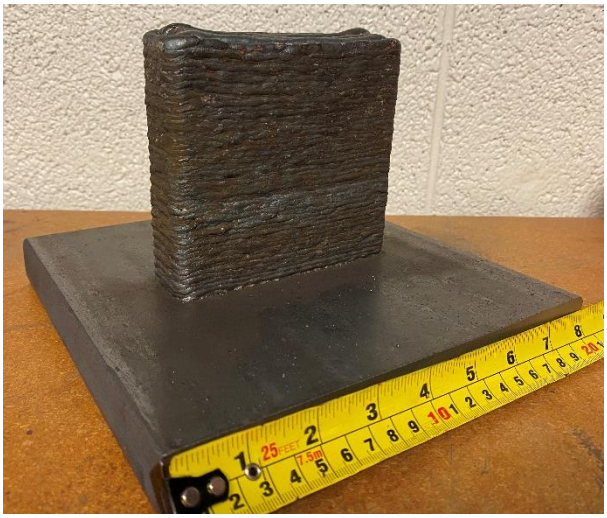

FIGURE 1. Wall preform as printed on a baseplate.

In this research, the focus is the digital twin information associated with the machining steps. This includes: 1) a structured light scan of the AM preform with temporary fiducials used to identify a local coordinate system; 2) selection of the cutting tool used to machine the preform; 3) measurements of the tool-holder-spindle-machine and preform frequency response functions, or FRFs, which describe their vibration

behavior; 4) the milling parameters, which include the axial and radial depths of cut, spindle speed, and feed per tooth values; 5) the tool paths generated by the CAM software; and 6) the machined part geometry and surface finish. For the purposes of demonstrating these steps a WAAM wall-shaped preform was printed on a steel baseplate with dimensions as shown in Fig. 1.

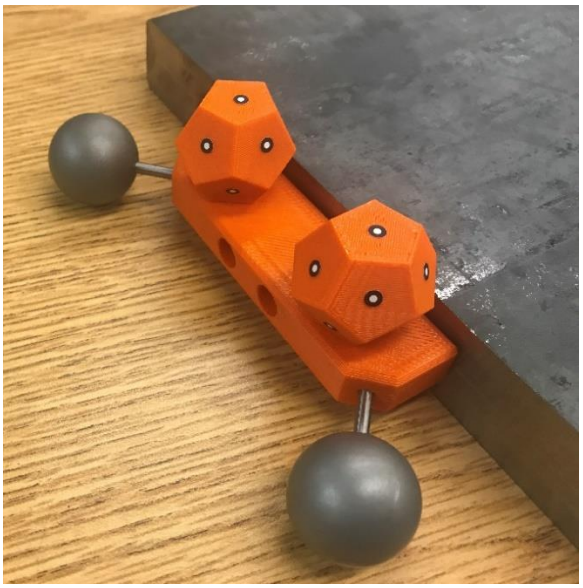

FIGURE 2. External fiducial apparatus that supports the fiducials (25.4 mm diameter, satin-finish spheres) and dodecahedron scan targets.

EXTERNAL FIDUCIAL APPARATUS

An external fiducial apparatus was designed and fabricated using fused filament fabrication (FFF) with ABS material. The apparatus volume is small to limit material use and avoid obscuring the preform during scanning, while remaining generic for use with various preform geometries. The fiducial apparatus serves two major purposes. First, it supports fiducials (tooling spheres in this case) that can be located in both the scan and in the milling machine. Second, it supports targets that the scanning software requires to maintain tracking across scans. Therefore, targets are not needed on the baseplate or part itself. The fiducial apparatus was attached via two threaded fasteners on both the left and right side of the baseplate; see Fig. 2. The left fiducial apparatus contained two spheres while the right contained only one sphere (not shown).

The fiducials were 25.4 mm diameter satin-finish spheres designed for optical scanning calibration (Bal-tec SAT-B100). The spheres were attached to the apparatus using press-fit dowel pins. Because it is necessary for the spheres to be accessible to both the structured light scanner (line-of-sight imaging) and the spindle-mounted probe on the milling machine, the fiducial apparatus was designed to hold the fiducials at a 45 degree angle to maximize probe access. It was not necessary to specifically locate the spheres since their positions are measured using the structured light scanner.

The scanning targets were placed on the faces of two dodecahedrons per fiducial apparatus (four total). The dodecahedron was chosen to provide multiple faces/targets at any viewing angle. The structured light scanning system used in this research (GOM ATOS Q) requires at least three targets to be in view from one scan to the next.

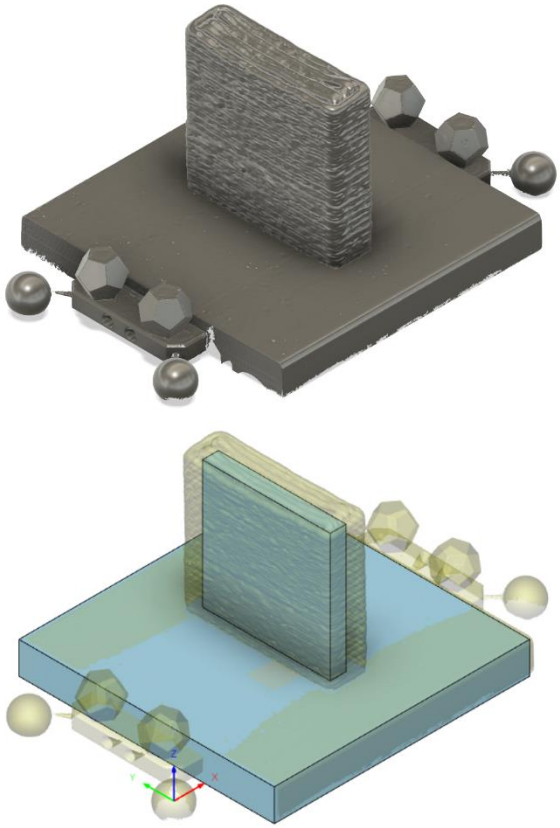

FIGURE 3. Scan of wall with attached fiducials (top). Alignment of wall geometry inside the preform (bottom).

SCAN TO CAM

An initial scan of the preform with fiducials is displayed in Fig. 3. The computer-aided design (CAD) digital preform model was aligned to the scan using the three planes of the base plate. The

final alignment of the scan to preform model is also shown in Fig. 3. This alignment was used to visually ensure that the preform model was fully contained within the scan (as-printed preform).

After the preform scan and model were aligned, the shared coordinate system was established. The coordinate system was defined kinematically based on a series of best-fit primitives [6]. The center of the first sphere was selected as the part origin, fixing three translational degrees of freedom. The bottom of the build plate was defined the Z axis, fixing two rotational degrees of freedom. The line between the centers of the first and second spheres (left and right front spheres in Fig. 3) defined the X axis, fixing the final rotational degree of freedom. The third sphere was redundant due to the build plate geometric constraint and was not used to define the coordinate system. The coordinate system is displayed in Fig. 3.

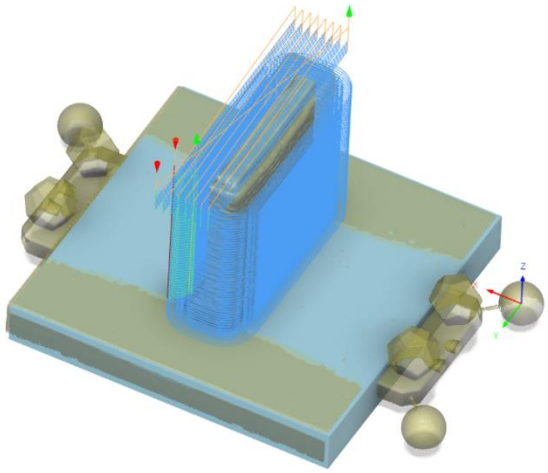

FIGURE 4. CAM toolpaths for wall machining.

Toolpaths were then defined relative to the established coordinate system within the CAM software (Fig. 4). The scan was imported directly as a stock model to enable full digital simulation. A snapshot of the simulation is shown in Fig. 5. This simulation, again, provided verification that the model was fully contained within the preform. Other benefits enabled by an accurate stock model include collision detection and the actual surface location for setting the initial radial depth of cut to engage the cutter the desired amount into the rough WAAM surface.

The preform was then loaded into a Haas VF-4 CNC milling machine and clamped to the table using a vise; this aligned the bottom of the baseplate to the machine table and defined the same Z axis direction for each. To fully relate the preform and machine coordinate systems, two tooling spheres (left and right front spheres in Fig. 3) were probed using the on-machine touch trigger probe and built-in routines to find the sphere centers. The line between these centers described the preform's X axis. A coordinate rotation about the Z axis was then performed to align the machining X direction with the preform X direction. No specific probing of the preform was required since the tooling spheres were already related to the preform location in the scan and, therefore, the CAM stock model used to generate the toolpaths.

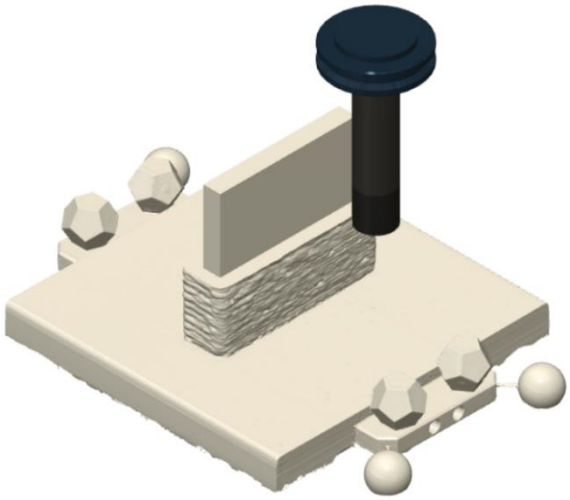

FIGURE 5. CAM simulation of wall machining.

MILLING PARAMETER SELECTION

A four flute, 25.4 mm diameter end mill with a 25.4 mm flute length (YG1 model UGMF73912) was used to machine the preform. The endmill had a 103 mm extension length from the tool holder and had a reduced shank diameter to enable machining of the full wall height. To determine optimum milling parameters a tap test was performed both at the tool's free end and the preform's top corner to measure the frequency response functions, or FRFs. Figure 6 shows that the tool was much less stiff (i.e., larger amplitudes in the real and imaginary parts of the complex-valued FRFs) than the preform and therefore dominated the selection of stable milling parameters. The tool and preform FRFs were then used to generate the corresponding stability maps (Fig. 7), where the specific cutting force for the steel preform was 1985 N/mm^2. An initial axial depth of cut of 2 mm and spindle speed of 5300

rpm were selected to obtain stable (chatter-free) cutting conditions. The corresponding surface speed was 422.9 m/min and the feed per tooth was 0.026 mm

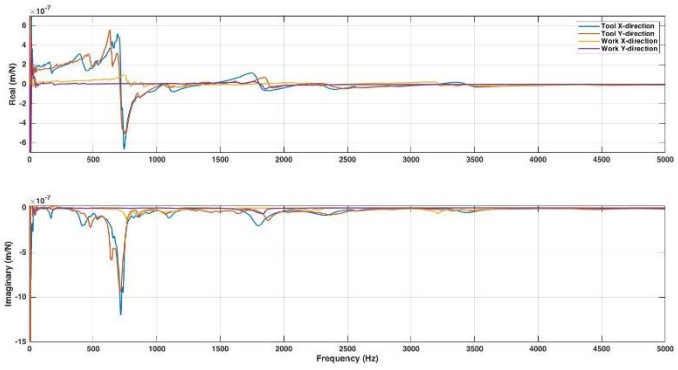

FIGURE 6. Real and imaginary parts of the tool and preform FRFs in the X and Y directions.

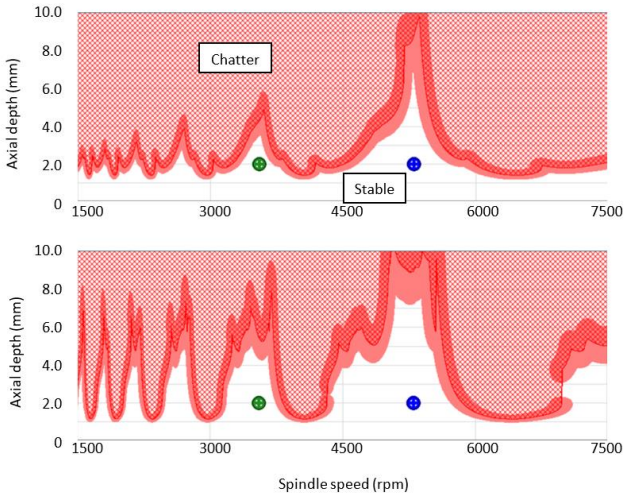

FIGURE 7. Stability map for X direction milling (top). Stability map for Y direction milling (bottom). The blue marker designates the parameters for the initial 10 mm of material removal (near the perform top). The green marker designates the parameters for the remaining preform height.

The machining process consisted of two primary operations completed in a single setup. First, the perform top was faced. Second, the perform sides were machined. The top facing nominally consisted of four axial steps down; however, an extra step was added due to the discovery of internal voids created by the WAAM process. This reduced the wall's final height by 2 mm. The side milling operations included three radial steps: 3.05 mm radial depth to clean up the preform's initial rough surface; 5.08 mm to remove the bulk of the material; and 2.54 mm for the final pass. A photograph of the preform after facing the top and completing a few axial steps down the perform sides is provided in Fig. 8.

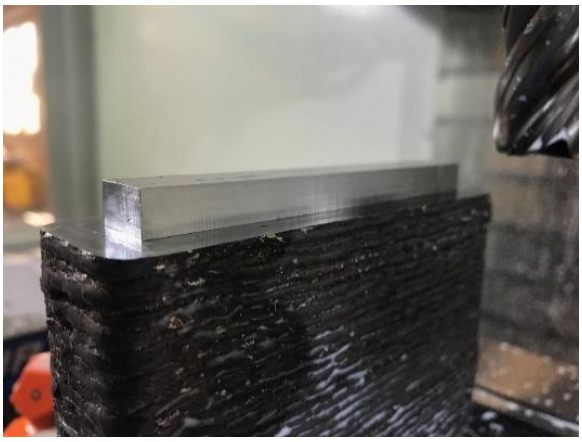

FIGURE 8. Photograph during preform milling.

At a height of 10 mm from the preform top, the spindle speed was reduced to 3550 rpm since initial wear was observed on the endmill. The reduced cutting speed (283.3 m/min) decreased the wear rate and enabled the wall to the finished, while retaining stable cutting conditions. This second selected point is also identified in the Fig. 7 stability maps.

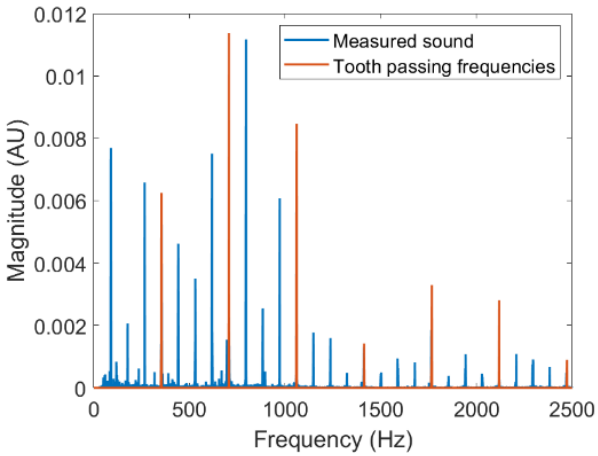

FIGURE 9. Frequency content of sound signal measured during milling at the preform top (5300 rpm).

To verify that the machining conditions were stable, audio data was recorded during machining and the frequency content was evaluated; see Fig. 9. It is observed that the measured sound occurs at the tooth passing

frequency (spindle speed multiplied by the number of teeth), integer multiples of the tooth passing frequency, or runout frequencies (spindle speed and integer multiples). A photograph of the wall after machining is displayed in Figure 10.

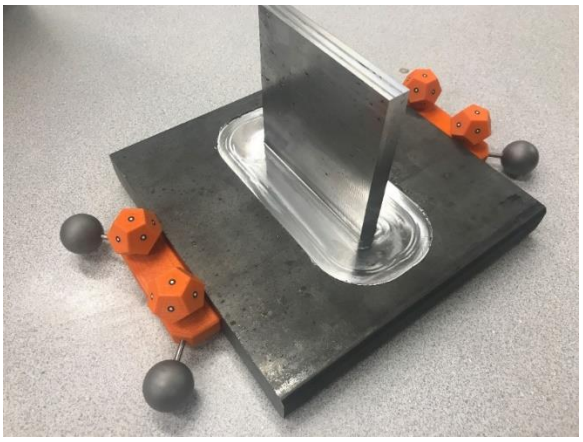

FIGURE 10. Wall geometry after milling. The fiducials are still attached to baseplate.

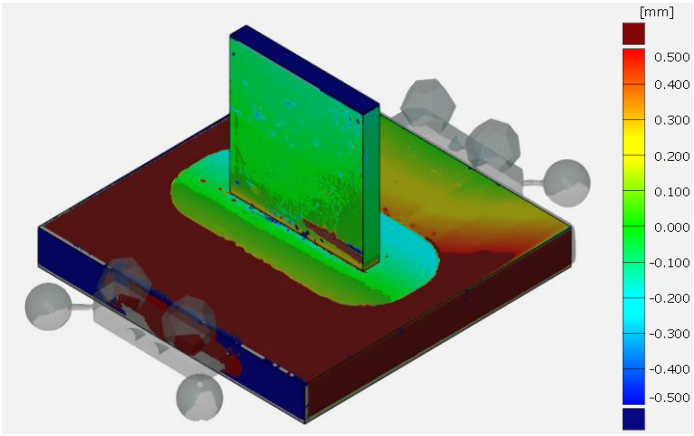

FIGURE 11. Surface deviation between the as-machined scan and the CAD model.

POST-MACHINING MEASUREMENTS

Further measurements were completed after machining to verify the size, shape, and surface finish of the wall. First, a scan was completed of the wall with the fiducials still attached. A surface deviation plot was created in comparison to the intended CAD model; see Fig. 11. Note that the top of the wall shows an error of over 0.5 mm due to the additional facing step completed at the wall top (not originally modeled in CAD). Other significantly negative values are due to voids left by the WAAM process. Positive readings are attributed to tool wear, which exceeded 0.6 mm flank wear width at the end of the cut; see Fig. 12.

FIGURE 12. Tool wear on the most worn relief face after machining.

A stylus profilometer was used to further examine the machined surface. Average roughness (Ra) measurements were performed in the feed direction (Y) at various Z heights in the YZ plane; see Figure 13. These Ra values agree with the expected surface roughness for the selected feed per tooth.

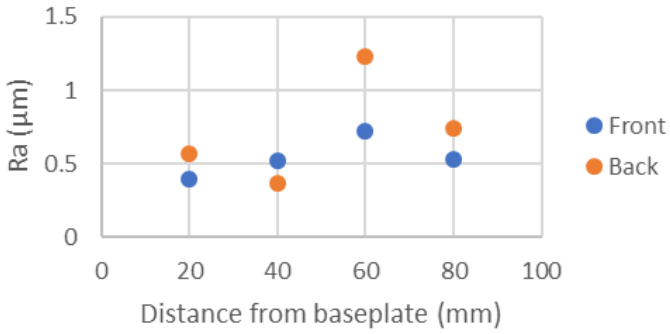

FIGURE 13. Average roughness for selected locations on wall sides.

DISCUSSION

This work demonstrates the value of a digital twin for machining operations in hybrid manufacturing. The combination of the fiducial apparatus and structured light scanning provide not only an accurate stock model, but also a connection between the preform and machine coordinate systems. This reduces setup time on the CNC machining center, confirms that the desired part geometry is contained within the as-printed preform for the machining orientation, and enables accurate CAM simulation of the toolpaths.

Measurement of the preform and tool tip FRFs enables selection of machining parameters that provide stable cutting conditions which respect

the limitations imposed by the process dynamics, while obtaining the highest possible metal removal rate and, therefore, highest process efficiency. Similarly, by considering the preform dynamics, the initial preform design can be informed (or modified) to ensure that the preform does not significantly reduce metal removal rates due to low dynamic stiffness. This can be a natural outcome of "too near-net" shape designs.

While measuring the preform and tool tip dynamics enables the pre-process selection of stable cutting parameters with high productivity, tool wear and measurement uncertainties can lead to uncertainty in the stability map. Therefore, in-process signals, such as the audio signal during machining, can serve to augment the predictions and identify unwanted outcomes, such as chatter.

Post-machining part measurements are used to confirm that the intended geometry, surface finish, and dynamics are achieved. In this case, a stylus profilometer was used, although optical methods are also available. Tap testing may also be used to identify natural frequencies, modal stiffness and damping ratio values, and mode shapes of the machined part. FEA comparisons may be completed for comparison.

Collectively, these components form the machining digital twin for hybrid manufacturing. Further work to test this digital twin methodology will include increasingly complex preform and CAD model geometries. This will test the robustness of the methodology while providing further detail on the "manual" step of aligning the stock model and CAD model.

CONCLUSIONS

In this paper, multiple aspects of a machining digital twin for hybrid manufacturing were shown. Temporary fiducials were attached to a WAAM preform and scanned via structured light to define a local coordinate system and CAM stock model. The WAAM preform and tool were tap tested to generate a stability map for the machining process, allowing for tool and milling parameter selection, including axial and radial depths of cut, spindle speed, and feed per tooth. Audio was recorded during machining and surface profilometry was completed post-machining to validate the absence of chatter and expected surface finish. A structured light scan of the final part was taken to compare to the CAD model. The proposed machining digital twin provided an accurate model for the machining process as demonstrated by validation experiments.

ACKNOWLEDGEMENTS

This work relates to Department of Navy award (ONR Award No. N00014-20-1-2836) issued by the Office of Naval Research. The United States Government has a royalty-free license throughout the world in all copyrightable material contained herein.

This manuscript has been authored by UT-Battelle, LLC, under contract DE-AC05-00OR22725 with the US Department of Energy (DOE). The US government retains and the publisher, by accepting the article for publication, acknowledges that the US government retains a nonexclusive, paid-up, irrevocable, worldwide license to publish or reproduce the published form of this manuscript, or allow others to do so, for US government purposes. DOE will provide public access to these results of federally sponsored research in accordance with the DOE Public Access Plan (http://energy.gov/downloads/doe-public-access-plan).

REFERENCES

1. Schmitz, T. and Smith, K.S., 2019, Machining Dynamics: Frequency Response to Improved Productivity, Second Edition, Springer, New York, NY.
2. Tuegel, E.J., Ingraffea, A.R., Eason, T.G. and Spottswood, S.M., 2011. Reengineering aircraft structural life prediction using a digital twin. International Journal of Aerospace Engineering, 2011.
3. Shafto, M., Conroy, M., Doyle, R., Glaessgen, E., Kemp, C., LeMoigne, J. and Wang, L., 2012. Modeling, simulation, information technology & processing roadmap. National Aeronautics and Space Administration, 32, pp.1-38.
4. Grieves, M., 2014. Digital twin: manufacturing excellence through virtual factory replication. White paper, 1, pp.1-7.
5. Boschert, S. and Rosen, R., 2016. Digital twin—the simulation aspect. In Mechatronic futures (pp. 59-74). Springer, Cham.
6. Smith, S.T., Chetwynd, DG., 1992. Foundations of Ultraprecision Mechanism Design. Gordon and Breach Science Publishers, Belgium.